J|A|C|S ARTICLES

Published on Web 12/09/2008

NMR Characterization of Fourth-Generation PAMAM Dendrimers in the Presence and Absence of Palladium Dendrimer-Encapsulated Nanoparticles

M. Victoria Gomez,[†] Javier Guerra,[‡] Aldrik H. Velders,*[,†] and Richard M. Crooks*[,‡]

NMR & MS Department, SupraMolecular Chemistry and Technology, MESA+ Institute for Nanotechnology, Faculty of Science and Technology, University of Twente, P.O. Box 217, 7500 AE Enschede, The Netherlands, and the Department of Chemistry and Biochemistry, Center for Nano and Molecular Science and Technology, and the Texas Materials Institute, The University of Texas at Austin, 1 University Station, A5300, Austin, Texas 78712-0165

Received September 20, 2008; E-mail: a.h.velders@utwente.nl; crooks@cm.utexas.edu

Abstract: High-resolution solution NMR spectroscopy has been used to characterize the structure of Pd dendrimer-encapsulated nanoparticles (DENs), consisting of approximately 55-atom nanoparticles encapsulated within fourth-generation, hydroxyl-terminated poly(amidoamine) PAMAM dendrimers (G4-OH). Detailed analysis of 1D and 2D NMR spectra of dendrimers with (G4-OH(Pd_{55})) and without (G4-OH) nanoparticles unambiguously demonstrate that single nanoparticles are encapsulated within individual dendrimers. This conclusion is based on the following results. First, the NMR data show that signals arising from the innermost methylenes of G4-OH(Pd_{55}) are more highly influenced by the presence of the Pd nanoparticles than are the terminal functional groups. This means that DENs are encapsulated within dendrimers rather than being adsorbed to their surface, as would be the case for aggregates consisting of multiple dendrimers and nanoparticles. Second, extraction of DENs from within their dendrimer hosts results in an increase in the NMR intensity associated with the interior methylenes, which corroborates the previous point. Third, NMR pulse-field gradient spin−echo experiments demonstrate that G4-OH and G4-OH(Pd_{55}) have identical hydrodynamic radii, and this finding excludes the presence of dendrimer/nanoparticle aggregates.

Introduction

We report the use of high-resolution, solution NMR spectroscopy to better understand the properties of fourth-generation, hydroxyl-terminated poly(amidoamine) (PAMAM) dendrimers (G4-OH) in the presence and absence of Pd dendrimer-encapsulated nanoparticles (DENs).[1] NMR spectra of G4-OH dendrimers and the corresponding 55-atom Pd DENs (G4-OH(Pd_{55})) appear nearly identical, but a detailed analysis of 1D and 2D NMR data provides compelling evidence for encapsulation of the nanoparticles inside the dendritic voids. Specifically, compared to G4-OH, proton signals arising from functional groups within the innermost four generations of G4-OH(Pd_{55}) have lower intensities. However, intensities arising from the outermost functional groups on the peripheries of G4-OH and G4-OH(Pd_{55}) are the same. Moreover, the results of pulsed-field gradient spin−echo (PFGSE) NMR experiments indicate that the diffusion coefficients of G4-OH dendrimers with and without encapsulated Pd nanoparticles are very similar, which also indicates nanoparticle encapsulation. Finally, 2D NMR experiments, including $^1H-^{13}C$ and $^1H-^{15}N$ heteronuclear multiple-bond correlation (HMBC) and heteronuclear single-bond correlation ($^1H-^{13}C$ HSQC), also yield similar spectra for G4-OH and G4-OH(Pd_{55}). Taken together, the results presented here provide spectroscopic evidence that Pd nanoparticles are encapsulated within individual G4-OH dendrimers and that their chemical interaction with the dendrimer is relatively weak.

PAMAM dendrimers have been used by us[1] and others[2−7] as a template for the synthesis of monometallic,[1,8−13] as well as alloy[1,11,14] and core/shell[1,14] bimetallic, nanoparticles containing up to a few hundred atoms. The synthetic method for preparing DENs depends on the identity of the metal, but it is generally carried out in two steps. First, metal ions are introduced to a solution of dendrimers, which results in complexation of the ions by interior tertiary amines of the dendrimer. Second, the encapsulated metal ions are chemically reduced, which results in formation of metallic DENs. Because the dendrimer acts as a template, DENs are often nearly monodisperse in size, composition, and structure. Note, however, that

[†] University of Twente.
[‡] The University of Texas at Austin.

(1) Scott, R. W. J.; Wilson, O. M.; Crooks, R. M. *J. Phys. Chem. B* **2005**, *109*, 692–704.
(2) Lang, H.; Chandler, B. D. *Nanotechnology in Catalysis*; Springer, 2007; Vol. 3.
(3) Chandler, B. D.; Gilbertson, J. D. *Top. Organomet. Chem.* **2006**, *20*, 97–120.
(4) Gröhn, F.; Bauer, B. J.; Akpalu, Y. A.; Jackson, C. L.; Amis, E. J. *Macromolecules* **2000**, *33*, 6042–6050.
(5) Lang, H.; Maldonado, S.; Stevenson, K. J.; Chandler, B. D. *J. Am. Chem. Soc.* **2004**, *126*, 12949–12956.
(6) Ozturk, O.; Black, T. J.; Perrine, K.; Pizzolato, K.; Williams, C. T.; Parsons, F. W.; Ratliff, J. S.; Gao, J.; Murphy, C. J.; Xie, H.; Ploehn, H. J.; Chen, D. A. *Langmuir* **2005**, *21*, 3998–4006.
(7) Chung, Y.-M.; Rhee, H.-K. *J. Mol. Catal. A: Chemical* **2003**, *206*, 291–298.

although the DENs used in this study are denoted as G4-OH(Pd_{55}), they are not perfectly monodisperse in size: the subscript refers to the ratio of Pd^{2+}:G4-OH used in the synthesis, not to the exact number of atoms in each nanoparticle. Finally, DENs are good model catalysts, because the dendrimers are highly permeable and do not fully passivate the surface of the encapsulated nanoparticles.[15]

There is much circumstantial evidence suggesting that DENs reside within dendrimeric voids. For example, transmission electron microscopy (TEM) studies have provided visual evidence of the association of Au DENs with high-generation PAMAM dendrimers.[4] More recently, extended X-ray absorption fine-structure (EXAFS) spectroscopy studies of monometallic Au and bimetallic PdAu DENs have suggested minimal interaction between DENs and the encapsulating dendrimeric host.[14,16] Additional indications for encapsulation come from numerous studies indicating that the dendrimer is able to modulate the solubility[1] and catalytic activity of DENs.[1,12,15] Results showing that DENs can be extracted from within dendrimers,[1] in the form of monolayer-protected clusters (MPCs),[17] are also consistent with DEN encapsulation. However, NMR provides a direct spectroscopic probe of perturbations to functional groups within the dendrimer, which are close to the encapsulated nanoparticle, and therefore it can provide particularly persuasive confirmation of the DEN location.

NMR has been an important tool for characterizing the structure[18−22] and physical properties[23] of dendrimers. For example, NMR has been used to elucidate diffusion coefficients (using PFGSE NMR),[24,25] interior mechanics,[26−29] free volume (using ^{129}Xe NMR),[30] self-assembly,[31] and the nature of the interactions between interior functional groups and metal ions.[32] With regard to the latter point, Pellechia et al. performed a ^{195}Pt NMR study to better understand interactions between Pt complexes and PAMAM dendrimers.[33] They discovered a time-dependent decrease in the Pt signal intensity, which was interpreted in terms of chelation of Pt^{2+} deep within the dendrimers. However, they did not perform an NMR study of the dendrimer/metallic-nanoparticle composite after reduction.

Here, we present an NMR spectroscopic study, which includes ^{1}H NMR, 2D-homonuclear correlation spectroscopy (COSY), ^{1}H−^{13}C heteronuclear single quantum coherence (HSQC), ^{1}H−^{13}C heteronuclear multiple bond correlation (HMBC), and ^{1}H−^{15}N HMBC, of G4-OH, G4-OH complexed to approximately 55 Pd^{2+} ions (G4-OH(Pd^{2+})$_{55}$), and G4-OH(Pd^{2+})$_{55}$ after reduction with BH_4^- (G4-OH(Pd_{55})). The key findings are as follows. First, the ^{1}H NMR spectra of G4-OH and G4-OH(Pd_{55}) show identical chemical shift values, with only a slight increase in the line widths for G4-OH(Pd_{55}). In contrast, the ^{1}H NMR spectrum of G4-OH(Pd^{2+})$_{55}$ reveals much broader peaks, owing to the decrease in symmetry introduced by the presence of coordinated Pd^{2+} ions. Second, the relative integrals of the signals from protons within the dendrimer interior and on the dendrimer periphery change upon encapsulation of the nanoparticle, the former decreasing more than the latter. Third, upon addition of thiol modifiers to the DENs, the signals of the interior dendrimer protons regain their relative intensities indicating extraction of the nanoparticles. Fourth, PFG experiments show that the diffusion coefficients of G4-OH and G4-OH(Pd_{55}) are nearly identical, indicating that the DEN is associated with the dendrimer in a way that does not change the size (hydrodynamic radius) of the dendrimer host. That is, each nanoparticle is associated with a single dendrimer, and no dendrimer-stabilized nanoparticles (DSNs, multiple dendrimers surrounding a single nanoparticle)[34] are observed.

Experimental Section

Chemicals. G4-OH was purchased as a 10.2 wt% methanol solution (Dendritech, Inc., Midland, MI). The methanol was removed under vacuum prior to use, and deuterated water or 18 MΩ·cm Milli-Q deionized water (Millipore) was added to obtain aqueous solutions of G4-OH having the desired concentrations. K_2PdCl_4, $NaBH_4$ (99.9%, Reagent Plus), 2-mercaptoethanol, and D_2O (99.999%) (Sigma-Aldrich, Inc.) were used as received. All experiments were carried out in air unless otherwise specified.

Synthesis of Pd DENs. Pd DENs for experiments other than those involving NMR studies were prepared according to previous reports.[35,36] Briefly, 1.10 mL of a freshly prepared, aqueous 10.0 mM K_2PdCl_4 solution was added to a 10.0 μM (final concentration) aqueous G4-OH solution (18.79 mL). The metal complex/dendrimer solution was stirred in a closed vial for 5 min to allow Pd^{2+} to

(8) Knecht, M. R.; Weir, M. G.; Myers, V. S.; Pyrz, W. D.; Ye, H.; Petkov, V.; Buttrey, D. J.; Frenkel, A. I.; Crooks, R. M. *Chem. Mater.* **2008**, *20*, 5218–5228.
(9) Garcia-Martinez, J. C.; Lezutekong, R.; Crooks, R. M. *J. Am. Chem. Soc.* **2005**, *127*, 5097–5103.
(10) Wilson, O. M.; Knecht, M. R.; Garcia-Martinez, J. C.; Crooks, R. M. *J. Am. Chem. Soc.* **2006**, *128*, 4510–4511.
(11) Ye, H.; Crooks, R. M. *J. Am. Chem. Soc.* **2007**, *129*, 3627–3633.
(12) Ye, H.; Crooks, R. M. *J. Am. Chem. Soc.* **2005**, *127*, 4930–4934.
(13) Knecht, M. R.; Crooks, R. M. *New J. Chem.* **2007**, *31*, 1349–1353.
(14) Knecht, M. R.; Weir, M. G.; Frenkel, A. I.; Crooks, R. M. *Chem. Mater.* **2008**, *20*, 1019–1028.
(15) Crooks, R. M.; Lemon, B. I., III.; Sun, L.; Yeung, L. K.; Zhao, M. *Top. Curr. Chem.* **2001**, *212*, 81–135.
(16) Petkov, V.; Bedford, N.; Knecht, M. R.; Weir, M. G.; Crooks, R. M.; Tang, W.; Henkelman, G.; Frenkel, A. I. *J. Phys. Chem. C* **2008**, *112*, 8907–8911.
(17) Templeton, A. C.; Wuelfing, W. P.; Murray, R. W. *Acc. Chem. Res.* **2000**, *33*, 27–36.
(18) Caminade, A.-M.; Laurent, R.; Majoral, J.-P. *Adv. Drug Delivery Rev.* **2005**, *57*, 2130–2146.
(19) Rinaldi, P. L. *Analyst* **2004**, *129*, 687–699.
(20) Shi, X.; Lesniak, W.; Islam, M. T.; Mu∼niz, M. C.; Balogh, L. P.; Baker, J. R., Jr. *Colloids Surf. A* **2006**, *272*, 139–150.
(21) Tomalia, D. A.; Baker, H.; Dewald, J.; Hall, M.; Kallos, G.; Martin, S.; Roeck, J.; Ryder, J.; Smith, P. *Polym. J.* **1985**, *17*, 117–132.
(22) Deloncle, R.; Coppel, Y.; Rebout, C.; Majoral, J.-P.; Caminade, A.-M. *Magn. Reson. Chem.* **2008**, *46*, 493–496.
(23) Langereis, S.; Dirksen, A.; Hackeng, T. M.; van Genderen, M. H. P.; Meijer, E. W. *New J. Chem.* **2007**, *31*, 1152–1160.
(24) Fritzinger, B.; Scheler, U. *Macromol. Chem. Phys.* **2005**, *206*, 1288–1291.
(25) Sagidullin, A.; Fritzinger, B.; Scheler, U.; Skirda, V. D. *Polymer* **2004**, *45*, 165–170.
(26) Malyarenko, D. I.; Vold, R. L.; Hoatson, G. L. *Macromolecules* **2000**, *33*, 7508–7520.
(27) Malyarenko, D. I.; Vold, R. L.; Hoatson, G. L. *Macromolecules* **2000**, *33*, 1268–1279.
(28) Meltzer, A. D.; Tirrell, D. A.; Jones, A. A.; Inglefield, P. T. *Macromolecules* **1992**, *25*, 4549–4552.
(29) Meltzer, A. D.; Tirrell, D. A.; Jones, A. A.; Inglefield, P. T.; Hedstrand, D. M.; Tomalia, D. A. *Macromolecules* **1992**, *25*, 4541–4548.
(30) Morgan, D. R.; Stejskal, E. O.; Andrady, A. L. *Macromolecules* **1999**, *32*, 1897–1903.
(31) Menger, F. M.; Peresypkin, A. V.; Wu, S. *J. Phys. Org. Chem.* **2001**, *14*, 392–399.
(32) Krot, K. A.; Danil de Namor, A. F.; Aguilar-Cornejo, A.; Nolan, K. B. *Inorg. Chim. Acta* **2005**, *358*, 3497–3505.
(33) Pellechia, P. J.; Gao, J.; Gu, Y.; Ploehn, H. J.; Murphy, C. J. *Inorg. Chem.* **2004**, *43*, 1421–1428.
(34) Garcia, M. E.; Baker, L. A.; Crooks, R. M. *Anal. Chem.* **1999**, *71*, 256–258.
(35) Zhao, M.; Crooks, R. M. *Angew. Chem., Int. Ed.* **1999**, *38*, 364–366.
(36) Scott, R. W. J.; Ye, H.; Henriquez, R. R.; Crooks, R. M. *Chem. Mater.* **2003**, *15*, 3873–3878.

fully complex with interior amines of the dendrimers (for simplicity, we denote $PdCl_4^{2-}$ and all of its hydrolysis products as Pd^{2+}).[36] Next, a 10-fold molar excess (0.11 mL) of freshly prepared, aqueous 1 M $NaBH_4$ was added to this precursor solution, and then the vial was sealed. Reduction occurs almost immediately to yield 20.0 mL of a 10.0 μM G4-OH(Pd_{55}) DEN solution.

The procedure used to prepare the DEN solutions for the NMR studies was slightly different from the one described in the previous paragraph, because the NMR experiments necessitated the use of small volumes. Specifically, 82.5 μL of a freshly prepared 10.0 mM K_2PdCl_4 solution in D_2O was added to a D_2O solution of G4-OH (0.015 μmol) to make a final volume of 1.5 mL. This resulted in a Pd^{2+}/G4-OH ratio of 55. The solution was stirred for 5 min, and then an aliquot of 600 μL was removed and used for ^{1}H NMR experiments. A freshly prepared 0.1 M D_2O solution of $NaBH_4$ (82.5 μL) was added to the just-described G4-OH(Pd^{2+})$_{55}$ solution to yield the DENs, and a 600 μL aliquot of this solution was used to perform the NMR experiments. A 2 mM D_2O solution of dioxane (0.01 mL) was used as internal standard. For extraction of DENs with 2-mercaptoethanol, 1.5 mL of a 10.0 μM aqueous G4-OH(Pd_{55}) solution were introduced into a 4 mL vial. Next, appropriate volumes of a 0.06 M 2-mercaptoethanol solution in D_2O (100 or 200 equiv, with respect to the dendrimer) were added. Finally, the NMR spectra (600 μL) were recorded after 5 min of stirring. 1D-, 2D-, and pseudo-2D NMR experiments were performed on 1 μM to 1 mM dendrimer solutions. If not specified otherwise in the text, the experiments were performed on 10 μM solutions. High-quality deuterated water (D_2O, 99.999%) was used for all measurements.

Peak assignments for G4-OH and G4-OH(Pd_{55}) were obtained using solutions containing 1 mM and 100 μM dendrimer, respectively. ^{1}H NMR (600.13 MHz, D_2O) δ(ppm): 3.57 (t, 128H, $^3J_{H,H}$ = 5.5 Hz, H_D), 3.25 (t, 128H, $^3J_{H,H}$ = 5.5 Hz, H_C), 3.23 (br t, 120H, H_c), 2.75 (br t, 128H, H_A), 2.74 (br t, 120H, H_a), 2.56 (br t, 120H, H_d), 2.36 (t, 128H, $^3J_{H,H}$ = 5.5 Hz, H_B), 2.34 (br t, 120H, H_b). ^{13}C NMR (150.03 MHz, D_2O) δ (ppm): 174.9 (64C, $-CO_t-$), 174.5 (60C, $-CO_b-$), 59.8 (64C, C_D), 51.2 (60C, C_d), 49.0 (124C, $C_{A/a}$), 41.4 (64C, C_C), 36.6 (60C, C_c), 32.6 (124C, $C_{B/b}$). ^{15}N NMR (60.81 MHz, D_2O) δ (ppm): 121.4 ($-CONH_b-$), 119.8 ($-CONH_t-$), 38.4 ($-N_b-$), 38.1 ($-N_t-$).

Characterization. TEM images were obtained using a JEOL-2010F TEM operating at 200 kV. Samples were prepared by dropwise (8 μL) addition of the sample onto a carbon-coated Cu grid (EM Sciences, Gibbstown, NJ) followed by solvent evaporation in air.

The NMR experiments were carried out using a Bruker Avance II NMR spectrometer operating at 600.13 MHz for ^{1}H, 150.03 MHz for ^{13}C, and 60.81 MHz for ^{15}N (14.1 T). The spectrometer was equipped with a Great 3/10 gradient amplifier and a triple-nucleus CP-TXI cryoprobe with a z-gradient. Cryogenic NMR probe technology can significantly increase the signal-to-noise ratio (*S*/*N*) of NMR spectroscopy,[37] which overcomes the limitation of low sensitivity[38] and makes it possible to study samples that aggregate at elevated concentration. High-quality 5 mm NMR tubes (pp-541, Wilmad LabGlass) were used to contain the dendrimer solutions (600 μL), and a presaturation pulse sequence was used to minimize the water peak in the 1D experiments. All 1D ^{1}H experiments (presaturation and homodecoupled) and 2D experiments (COSY, HMBC, HSQC) were performed at 300 K using standard pulse sequences from the Bruker library. Diffusion (PFGSE) NMR experiments were performed using the bipolar stimulated echo sequence with 32 increments in the gradient strength (2−95%), typically 16 averages per increment step, and 100 ms diffusion times. Pseudo-2D DOSY plots were processed with the standard Bruker software; the T1/T2 "vargrad" SimFit fitting routine

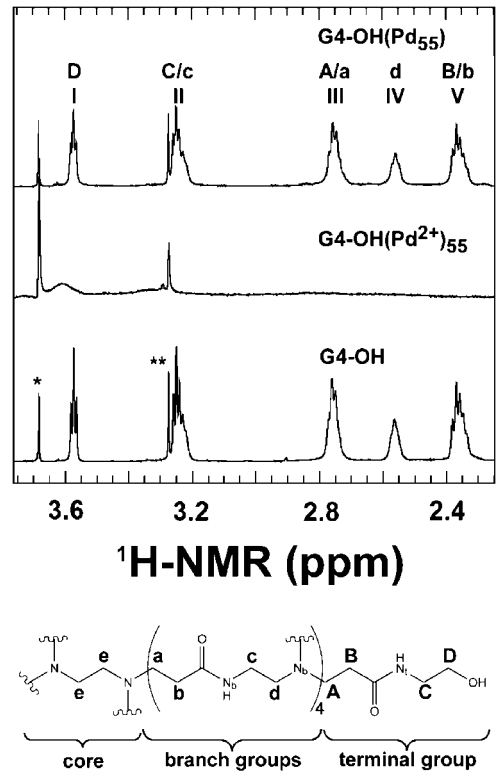

Figure 1. (Top) ^{1}H NMR spectra of G4-OH, G4-OH(Pd^{2+})$_{55}$, and G4-OH(Pd_{55}). The peak marked with a single asterisk arises from the dioxane internal standard, and the peak marked with a double asterisk arises from residual methanol. (Bottom) Schematic representation of G4-OH indicating the lettering scheme used to identify the methylene and nitrogen groups referred to in the manuscript.

was used to determine the diffusion coefficients. All NMR experiments were carried out using temperature control, which is necessary for cryoprobe experiments. PFGSE experiments were performed under tube-spinning conditions to limit convective transport arising from temperature gradients.[39] The gradient coil strength was calibrated on the diffusion peak of H_2O in D_2O (D = 19.2 × 10^{-10} m^2/s).[40]

Results and Discussion

The G4-OH PAMAM dendrimer is a macromolecule that contains over a thousand protons, and it has a molecular weight of ~15 kDa and an approximate diameter of 3.7 nm in methanol.[25] These factors conspire to make NMR characterization a challenge, but some simplifying assumptions can be made. For example, considering the structure and symmetry of G4-OH (Figure 1), it is reasonable to assume that all branch-group methylenes next to the tertiary amines are similar. That is, the *a*-group methylenes (Figure 1) have the same chemical shift in all four generations even though they are not all formally magnetically or chemically equivalent.[21] The same logic applies to methylenes *b*, *c*, and *d*. The terminal-group methylenes (*A*, *B*, *C*, and *D*), however, are closer to the hydroxyl end group than the corresponding methylenes in the branch groups, and therefore they might be expected to exhibit a (modestly) different chemical shift. This simplistic analysis of the structure of the G4-OH dendrimer suggests that only nine different methylene

(37) Styles, P.; Soffe, N. F.; Scott, C. A.; Cragg, D. A.; Row, F.; White, D. J.; White, P. C. J. *J. Magn. Reson.* **1984**, *60*, 397–404.
(38) Logan, T. M.; Murali, N.; Wang, G.; Jolivet, C. *Magn. Reson. Chem.* **1999**, *37*, 512–515.
(39) Lounila, J.; Oikarinen, K.; Ingman, P.; Jokisaari, J. *J. Magn. Reson., Ser. A* **1996**, *118*, 50–54.
(40) Martić, S.; Liu, X.; Wang, S.; Wu, G. *Chem. Eur. J.* **2008**, *114*, 1196–1204.

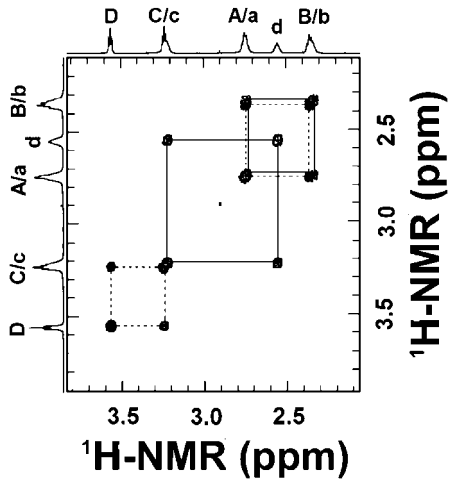

Figure 2. ^{1}H−^{1}H COSY spectrum of G4-OH. Cross peaks show the scalar coupling between the proton signals of the methylene group subunits. Dashed lines indicate the correlation of the terminal group units *A*/*B* and *C*/*D*, and solid lines indicate the correlation of the repeating unit groups of the four generations *a*/*b* and *c*/*d*.

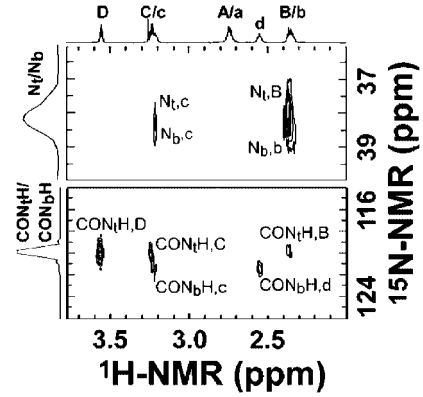

Figure 3. Expansion of the amine and amide peaks in the ^{1}H−^{15}N HMBC spectrum. Amines closest to the terminal groups (N_t) can be distinguished from the amines of the branches (N_b). Amides from the terminal groups (*CON$_t$H*) can be distinguished from the amides of the branches (*CON$_b$H*).

groups should be detected by ^{1}H NMR: the methylenes of the ethylenediamine core (methylenes *e*), those associated with the interior branch groups (methylene groups *a*, *b*, *c*, and *d*), and those of the terminal groups (methylene groups *A*, *B*, *C*, and *D*).

NMR Characterization of G4-OH. The bottom spectrum in Figure 1 was obtained from a 10.0 μM solution of G4-OH in D_2O. This ^{1}H NMR spectrum has a relatively simple appearance and only five peaks are observed (I, II, III, IV, and V). We assign proton signals I−V to the methylene protons of the dendrimer through a combination of 1D and 2D NMR experiments: ^{1}H, ^{1}H−^{1}H COSY (Figure 2), ^{1}H−^{15}N HMBC (Figures 3 and S1),^{1}H−^{13}C HSQC (Figure S2), and ^{1}H−^{13}C HMBC (Figure S3). Of the five main peaks in the 1D proton spectrum (Figure 1), two are triplets and three are broadened/overlapped peaks. Peak I (3.57 ppm) is a triplet attributable to methylene group *D*, the closest to the hydroxyl terminal group, and therefore expected to exhibit the most pronounced downfield shift with respect to all the other methylene groups (which are adjacent to a tertiary amine or amide group).

Peak II (3.25 ppm) consists of two overlapping peaks corresponding to methylene groups *C* and *c*. This assignment is based on two homonuclear correlation cross peaks in the ^{1}H−^{1}H COSY spectrum (Figure 2): one with peak I (group *D*) at 3.57 ppm and one with peak IV (and therefore attributed to group *d*) at 2.56 ppm. Because of these cross peaks, protons of methylenes *C* of the terminal group and the protons of inner methylenes *c* of the four generations of branch groups are distinguishable, the latter being slightly upfield shifted as observed in the ^{1}H−^{1}H COSY (Figure 2). The other cross peaks in the ^{1}H−^{1}H COSY (corresponding to peaks III and V) are due to couplings of methylenes *A*−*B* and *a*−*b*, respectively, which were assigned using the heteronuclear correlation spectra ^{1}H−^{15}N HMBC (Figures 3 and S1), ^{1}H−^{13}C HSQC (Figure S2), and ^{1}H−^{13}C HMBC (Figure S3).

From the ^{1}H−^{15}N HMBC data (Figures 3 and S1), which are focused on long-range (^3J and ^2J) proton−nitrogen interactions, two main cross peak areas are observed in the amine (37−39 ppm) and amide (116−124 ppm) regions. As for the proton spectra, these data make it possible to discriminate between the nitrogen signals of amines and amides arising from the branch and the terminal groups.

Analysis of the amide peak region (the most downfield region of the ^{1}H−^{15}N HMBC spectrum, 116−124 ppm, Figure 3), reveals two different types of amide groups: the amide groups in the terminal group (*CON$_t$H* at 119.8 ppm) and the amide groups in the branch groups (*CON$_b$H* at 121.4 ppm) of the four generations (Figures 3 and S1). In total, five cross peaks are observed in this region. The upfield shifted amide peak (119.8 ppm) corresponds to the amide of the terminal unit (*CON$_t$H*), as shown by the correlation peak with the *D* and *C* methylenes, while the more downfield shifted amide peak (121.4 ppm) corresponds to that of the four generations (*CON$_b$H*), as determined from the correlation peaks with the *d* and *c* methylenes. The fifth correlation peak (from the *CON$_t$H* groups to the proton peak at 2.35 ppm) leads to the unequivocal assignment of the *B* methylene groups (peak V in Figure 1).

Focusing now on the amine region (the most upfield shifted region at 37−39 ppm in the ^{1}H−^{15}N HMBC spectrum, Figure 3), only three cross peaks are observed. As for the amide signals, two types of amine groups can also be observed: the amine group located in the terminal group (N_t *at* 38.1 ppm) and the remaining amine groups located in the branch groups (N_b at 38.4 ppm). The former (38.1 ppm) gives a clear correlation peak with *c* that corroborates this assignment (see structure of dendrimer in Figure 1 and a more detailed view in Figure S1), as well as a cross peak with the *B* methylenes. Close analysis of the broad cross peak shows another correlation attributable to the *b* methylene groups, which are chemically and magnetically similar, but not identical, to *B*. These *b* methylenes exhibit a correlation with the tertiary amine groups of the branch groups (N_b), slightly downfield from the terminal group amine signal (N_t).

Peak III is the only one of the five proton signals not to exhibit cross peaks in the ^{1}H−^{15}N HMBC spectrum, and therefore it can be attributed to the *A* and *a* methylene group signals. The assignment of this peak is confirmed by two homonuclear correlation peaks in the ^{1}H−^{1}H COSY with peak V, previously assigned to *B*/*b* methylenes (Figure 2).

The heteronuclear ^{1}H−^{13}C HSQC (Figure S2) and ^{1}H−^{13}C HMBC (Figure S3) data complement the structural characterization of G4-OH. The correlation peaks observed in ^{1}H−^{13}C HSQC and in ^{1}H−^{13}C HMBC agree with the proton signal assignment made above. Interestingly, the $^{13}C_C$ and $^{13}C_c$ peaks

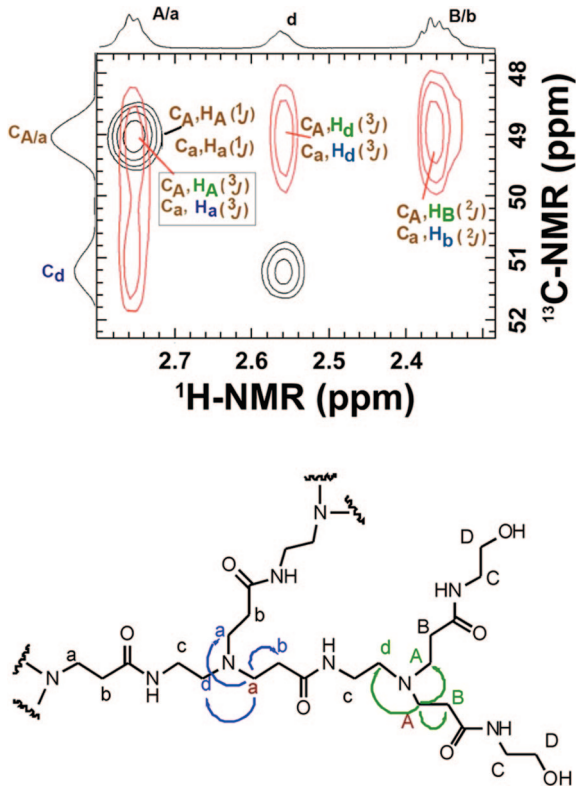

Figure 4. (Top) Expansion of overlapped $^1H-^{13}C$ HSQC (black) and $^1H-^{13}C$ HMBC (red) spectra for G4-OH, $^{13}C_{A/a}$-$^{13}C_d$, and $^1H_{A/a}-^1H_d-^1H_{B/b}$ region. Most remarkable are the C_A-H_A and C_a-H_a *long*-range (^3J) couplings, from the $C_{A/a}$ in one branch/unit to the H_A or H_a of an adjacent unit (highlighted in green and blue). (bottom) Arrows indicate $C_{A/a}-H_i$ couplings through two and three bonds (across the tertiary amine groups). Only $C_{A/a}$ connections are indicated in the spectra (top) and in the coupling scheme (bottom).

are separated by almost 5 ppm in the ^{13}C dimension of the $^1H-^{13}C$ HSQC, while the ^1H_C and ^1H_c peaks are severely overlapped (Figure S2).

Overlaid spectra of the $^1H-^{13}C$ HSQC and $^1H-^{13}C$ HMBC experiments reveal the typical complementary pattern for the ethylene units in the dendrimer of short-range and long-range couplings, respectively (Figures 4 and S4). The most remarkable feature in the HMBC experiment consists of a cross peak between C_A (49.0 ppm) and H_A (2.75 ppm) (HMBC, red cross peak Figures 4, S3, and S4), an unexpected peak at first sight as this cross peak is expected to be observed only in the HSQC experiment (HSQC, black cross peak in Figures 4, S2, and S4). Paradoxically, this most characteristic peak observed in the HMBC derives from the long-range (^3J) coupling of the C_A carbon to the H_A of *another* (symmetry-related magnetically and chemically equivalent) C_A, located in the adjacent branch at the other side of the tertiary amine (see dendrimer structure in Figure 4). Similarly, C_a (49.0 ppm) in the branch groups shows a (^3J) cross peak (red cross peak, Figure 4) with the H_a (2.74 ppm) at the symmetry-related branch connected to the adjacent tertiary amine, in addition to the (^1J) coupling (HSQC, black cross peak, Figure 4) to H_a (2.74 ppm).

In summary, the five ^1H NMR peaks of G4-OH shown in Figure 1 are assigned to the four methylene groups of the branch groups and the four methylenes of the terminal groups. The resonances of the pairs of methylene groups *A* and *a*, *B* and *b*, and *C* and *c* are strongly overlapped, and therefore each appears as one broad, partially resolved peak. In contrast, the *D* and *d* peaks are resolved into triplets. The signal arising from the core methylene groups (*e*) has not been identified for the following reasons. First, there are fewer core methylenes than in the branch or terminal groups, and hence the core intensity is much lower. Second, the peak from the core protons likely overlaps with the H_a-peak.[21] Third, the methylene protons in the core are likely to be affected by the restricted rotational movements of the dendritic branches causing intermittent symmetry disruption and corresponding broadening of the *e* signal.

The relative integrals of peaks I−V (Table 1 and Figure S5) are in satisfactory agreement with those expected based on the G4-OH structure. For example, the calculated ratio of the peak integrals corresponding to the *D* (peak I at 3.57 ppm) and *d* (peak IV at 2.56 ppm) methylene groups is 1.07 (128 protons of *D* methylenes/120 protons of *d* methylenes), and the experimentally determined ratio is 1.04 (Table 1, columns 7 and 9). The integral ratios between peak I (protons of *D* methylenes) and peak II (protons of methylenes $C + c$) is 0.54 (calculated: 128/248 = 0.52). Similar trends are observed for the other integral ratios.

NMR Characterization of G4-OH(Pd^{2+})$_{55}$. When $PdCl_4^{2-}$ and G4-OH are mixed in water, the former hydrolyzes and then complexes with functional groups within the dendrimer interior.[36,41−43] The G4-OH(Pd^{2+})$_{55}$ spectrum in Figure 1 shows how the ^1H NMR spectrum changes as a consequence of this reaction. The spectrum reveals two sharp peaks arising from 1,4-dioxane (3.68 ppm), which is used as an internal standard, and from methanol (3.27 ppm), which is a minor solvent impurity in the aqueous G4-OH solution. The loss of proton resonances after addition of Pd^{2+} is a consequence of the coordination of Pd^{2+} to (primarily) tertiary amines within the dendrimer.[36,33] Such behavior has previously been observed.[44−46] For example, Ooe et al. showed that the interaction of Pd^{2+} and poly(propylene imine) dendrimers (PPI) leads to broadening of the methylene signals α to the tertiary amines in ^1H NMR and the nitrogen signals of the tertiary amines in ^{14}N NMR.[44] A similar proton broadening effect was observed by Astruc and co-workers when Pd^{2+} ions interact with click dendrimers containing 1,2,3-triazole moieties.[45,46] This type of line broadening can be caused by a restricted conformation, which affects the relaxation time of the nuclei[33] or by the occurrence of fluxional processes arising from the presence of metallocycles.[47]

NMR Characterization of G4-OH(Pd_{55}). The G4-OH(Pd^{2+})$_{55}$ precursor complex was reduced by adding BH_4^-, and this resulted in the formation of G4-OH(Pd_{55}) DENs.[15] TEM analysis of these Pd DENs (Figure S6) indicates they have a size distribution of 1.2 ± 0.3 nm, which is consistent with previous results from our group and with the size calculated for cuboctahedral nanoparticles containing 55 Pd atoms.[1] NMR was used to achieve a better understanding of the structure of G4-

(41) Ye, H.; Scott, R. W. J.; Crooks, R. M. *Langmuir* **2004**, *20*, 2915–2920.
(42) Troitskii, S. Y.; Fedotov, M. A.; Likholobov, E. A. *Russ. Chem. Bull.* **1993**, *42*, 634–639.
(43) Elding, L. I.; Olsson, L. F. *J. Phys. Chem.* **1978**, *82*, 69–74.
(44) Ooe, M.; Murata, M.; Mizugaki, T.; Ebitani, K.; Kaneda, K. *Nano Lett.* **2002**, *2*, 999–1002.
(45) Ornelas, C.; Salmon, L.; Ruiz Aranzaes, J.; Astruc, D. *Chem. Commun.* **2007**, 4946–4948.
(46) Ornelas, C.; Aranzaes, J. R.; Salmon, L.; Astruc, D. *Chem.—Eur. J.* **2008**, *14*, 50–64.
(47) Diez-Barra, E.; Guerra, J.; Hornillos, V.; Merino, S.; Tejeda, J. *J. Organomet. Chem.* **2005**, *690*, 5654.

Table 1. Chemical Shifts, Integral Values, and Ratios for G4-OH and G4-OH(Pd_{55})

1	2	3	4	5	6	7	8	9
Principal Peak	Peaks	δ ^{1}H NMR (ppm)	I_{G4-OH}	$I_{G4-OH(Pd55)}$	$I_{G4-OH(Pd55)}/I_{G4\ OH}$	I_I/I_{I-V} G4–OH	I_I/I_{I-V} G4–OH(Pd_{55})	Calc. Values I_I/I_{I-V}
Footnote	a	b	c	d	e	f	f	g
I	*D* (128)	3.57	128	126	0.98±0.04	1	1	1
II	*C* (128)	3.25	238	213	0.89±0.04	0.54	0.59	0.52
	c (120)	3.23						
III	*A* (128)	2.75	246	210	0.85±0.04	0.52	0.60	0.52
	a (120)	2.74						
IV	*d* (120)	2.56	123	104	0.84±0.04	1.04	1.21	1.07
V	*B* (128)	2.36	250	207	0.83±0.04	0.51	0.61	0.52
	b (120)	2.34						

[a] (Number of protons.) [b] pH 9.9−9.6. [c] Integral values relative to peak I. [d] Integral values relative to dioxane, whose value has been calculated relative to peak I in G4-OH. [e] Integral ratio of G4-OH(Pd_{55})/G4-OH. [f] Integral ratio of peak I (D) to the other four peaks. [g] Calculated integral ratio of peak I (D) to the other four peaks.

OH(Pd_{55}) and, in particular, the spatial relationship between the (encapsulated) Pd nanoparticle and the dendrimer host.

The ^{1}H NMR spectrum of G4-OH(Pd_{55}) is very similar to that of G4-OH (Figure 1) in that the principal five peaks (I−V) corresponding to the dendrimer resonances re-emerge after reduction of G4-OH(Pd^{2+})$_{55}$. This suggests that the dendrimer is in approximately the same configuration with or without the encapsulated nanoparticle. The assignment of the proton peaks for the G4-OH(Pd_{55}) spectrum, carried out using ^{1}H−^{1}H COSY, ^{1}H−^{13}C HSQC, ^{1}H−^{13}C HMBC, and ^{1}H−^{15}N HMBC (Figures S7−S10), is in agreement with the analysis for G4-OH. The key question, however, is whether the spectrum of G4-OH(Pd_{55}) corresponds to the free dendrimer (no encapsulated Pd nanoparticle) or to the dendrimer carrying an encapsulated Pd nanoparticle within its interstitial voids. To address this question, we consider some slight differences between the spectra of G4-OH and G4-OH(Pd_{55}).

First, there is a minor upfield shift (<0.01 ppm) observed for peaks III (*A* + *a* methylenes) and IV (*d* methylenes) in the spectrum of G4-OH(Pd_{55}) compared to G4-OH. This upfield shift, however, results from the change in pH from 6.9 ± 0.2 to 9.7 ± 0.2 associated with the addition of BH_4^- to the solution.[48−50] This conclusion was confirmed by carrying out a control experiment in which G4-OH and $NaBH_4$ were mixed (in the absence of Pd^{2+}), showing that the G4-OH proton signals for this experiment closely correspond with those observed in the spectrum of G4-OH(Pd_{55}).

A second more significant difference is the slight decrease in the heights and broadening in the widths of all five peaks in the ^{1}H NMR spectrum of G4-OH(Pd_{55}) compared to the G4-OH spectrum. This effect can tentatively be attributed to local restricted motion and heterogeneity due to encapsulation of the nanoparticle. Similarly, in the case of MPCs, proton and carbon NMR signals of atoms of alkylthiols closer to the metallic nanoparticle are so broad that they are sometimes difficult to detect.[51−55] Note, however, that the interaction between thiols and gold nanoparticles is very strong, while the interaction between dendrimers and DENs is weak.[16]

The ratio of the peak integrals for G4-OH(Pd_{55}) relative to G4-OH were determined using the dioxane peak as an internal standard for normalizing the two spectra. Specifically, peak I in the G4-OH spectrum was calibrated to a value of 128 (number of protons associated with the *D* methylenes). Next, the dioxane integral value in the G4-OH spectrum was experimentally obtained taking into the account that the integral of peak I equals 128. Finally, this integral value for the dioxane peak was consecutively used as reference to normalize the G4-OH(Pd_{55}) spectrum. This approach makes it possible to directly compare the peak integrals of the G4-OH(Pd_{55}) and G4-OH spectra (columns 4, 5, and 6 of Table 1).

Interestingly, by determining the relative integrals with respect to the internal standard (1,4-dioxane, 3.68 ppm), it is clear that the ^{1}H-resonance intensity of peak I (*D* methylenes) is the same for G4-OH(Pd_{55}) and G4-OH (Table 1, column 6 and Figure S5). This means that the integral of peak I (terminal *D* methylenes) is nearly independent of the presence of the DEN, while the integral of peak IV (interior *d* methylenes) is

(48) Koper, G. J. M.; van Genderen, M. H. P.; Elissen-Roman, C.; Baars, M. W. P. L.; Meijer, E. W.; Borkovec, M. *J. Am. Chem. Soc.* **1997**, *119*, 6512–6521.
(49) Niu, Y.; Sun, L.; Crooks, R. M. *Macromolecules* **2003**, *36*, 5725–5731.
(50) Cakara, D.; Kleimann, J.; Borkovec, M. *Macromolecules* **2003**, *36*, 4201–4207.
(51) Lica, G. C.; Zelakiewicz, B. S.; Tong, Y. Y. *J. Electroanal. Chem.* **2003**, *554−555*, 127–132.
(52) Badia, A.; Demers, L.; Dickinson, L.; Morin, F. G.; Lennox, R. B.; Reven, L. *J. Am. Chem. Soc.* **1997**, *119*, 11104–11105.
(53) Badia, A.; Gao, W.; Singh, S.; Demers, L.; Cuccia, L.; Reven, L. *Langmuir* **1996**, *12*, 1262–1269.
(54) Hostetler, M. J.; Wingate, J. E.; Zhong, C. J.; Harris, J. E.; Vachet, R. W.; Clark, M. R.; Londono, J. D.; Green, S. J.; Stokes, J. J.; Wignall, G. D.; Glish, G. L.; Porter, M. D.; Evans, N. D.; Murray, R. W. *Langmuir* **1998**, *14*, 17–30.
(55) Terrill, R. H.; Postlethwaite, T. A.; Chen, C.-H.; Poon, C.-D.; Terzis, A.; Chen, A.; Hutchison, J. E.; Clark, M. R.; Wignall, G.; Londono, J. D.; Superfine, R.; Falvo, M.; Johnson, C. S., Jr.; Samulski, E. T.; Murray, R. W. *J. Am. Chem. Soc.* **1995**, *117*, 12537–12548.

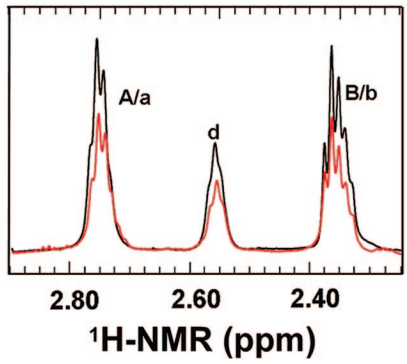

Figure 5. Comparison of the upfield region of G4-OH (black, same as G4-OH in Figure 1) and G4-OH(Pd_{55}) (red, same as G4-OH(Pd_{55}) in Figure 1) normalized to the dioxane internal standard. The assignment of the protons, with reference to the methylene groups shown in Figure 1, is indicated.

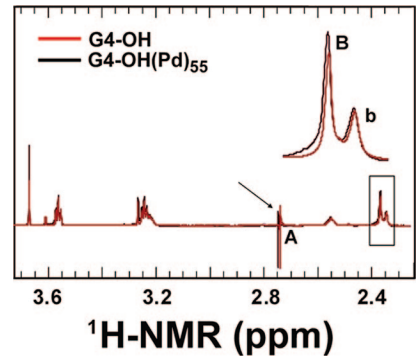

Figure 6. Comparison of the homodecoupled ^{1}H NMR spectra of G4-OH and G4-OH(Pd_{55}). The sample was irradiated at the *A*/*a* frequency (2.75 ppm). Spectra are normalized to the proton intensity of the *b* methylenes to emphasize the change in the *B*:*b* ratio.

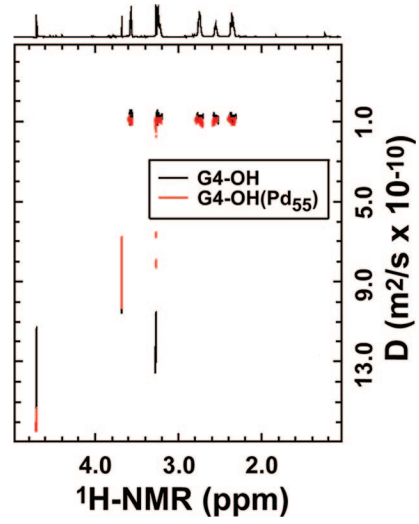

Figure 7. Comparison of the pseudo-2D DOSY plots for G4-OH(Pd_{55}) and G4-OH. Signals at 4.7, 3.7, and 3.3 ppm are water, dioxane, and methanol, respectively.

significantly lower (Figure 5 and column 6 of Table 1). In analogy to the reported NMR of MPCs,[51−55] and as discussed earlier, this observation suggests that the NMR signal from the interior *d* methylenes is reduced by the close proximity of the encapsulated DENs. A similar decrease in the intensity of peaks II, III, and V is observed in the presence of the DENs (Figure 5 and column 6 of Table 1). However, these latter three peaks arise from overlapping signals originating from both interior and terminal methylenes. Accordingly, it is not as straightforward to attribute the decrease of these signals to the presence of DENs as it is for peaks I and IV. However, as discussed next, it is possible to provide additional insight into the decrease of peak V.

We now turn our attention to the ratios of the measured and calculated peak integrals for G4-OH and G4-OH(Pd_{55}). Recall that these values, presented in columns 7, 8, and 9 of Table 1, correspond to the ratios of the integral of peak I to those of peaks I−V. In the absence of the DEN, the measured (column 7) and calculated (column 9) ratios for G4-OH are in good agreement. However, the measured ratios (column 8) are significantly larger than the calculated values (column 9) for G4-OH(Pd_{55}). Consistent with the discussion in the previous paragraph, this suggests loss of signal from the innermost methylene protons relative to the protons of terminal methylene *D*.

As discussed for G4-OH, it is also possible to discriminate between the chemical shifts of the interior methylenes (*a*, *b*, *c*) and the terminal methylenes (*A*, *B*, *C*) of G4-OH(Pd_{55}) despite the high degree of overlap. For *B* and *b* protons the integral intensity can also be compared by using a selective homodecoupling experiment. This experiment is carried out by irradiating on the proton resonances of the *A* and *a* methylenes (peak III), which eliminates the scalar coupling patterns in peak V (multiplets of the *B* and *b* methylenes). Figure 6 shows that this results in almost complete resolution of the signals arising from the *B* and *b* methylenes. The partial overlap of the peaks still complicates integration; however, it is possible to overlay the selectively homodecoupled spectrum of G4-OH and G4-OH(Pd_{55}) and normalize the heights of the interior *b* methylenes (inset of Figure 6). This operation shows that the *B*:*b* integral ratio determined for G4-OH(Pd_{55}) is significantly higher than that for G4-OH. This observation is in agreement with the earlier discussion of the peaks corresponding to the *D* and *d* methylene protons and is consistent with encapsulation of the DENs deep within the dendrimers. Unfortunately, the overlap and broadening in the *A* and *a* methylene resonances and the *C* and *c* are too severe ($\Delta\delta = 0.01$ ppm) to integrate the separate peaks from selective homodecoupling experiments.

Determination of Diffusion Coefficients of G4-OH and G4-OH(Pd_{55}) Using Pulsed-Field Gradient NMR. The foregoing discussion shows that 55-atom Pd DENs are encapsulated within G4-OH dendrimers. A prediction of this conclusion is that the diffusion coefficients of G4-OH and G4-OH(Pd_{55}) should be identical. That is, if the DENs are fully encapsulated within the dendrimers,[16] then the hydrodynamic radii of both G4-OH and G4-OH(Pd_{55}) will be the same and hence the diffusion coefficients should be about the same. Accordingly, we determined the diffusion coefficients of both species using PFGSE NMR experiments.

An advantage of cryoprobe NMR methods is that they enable measurements at low analyte concentration. This is particularly important for dendrimer solutions, which are known to aggregate at typical concentrations used for NMR spectroscopy.[24,25] Accordingly, the PFGSE NMR experiments described here were carried out using 10 μM G4-OH and G4-OH(Pd_{55}) solutions. The key finding is that the pseudo-2D plots for G4-OH and G4-OH(Pd_{55}) overlap (Figure 7), indicating that they have the same diffusion coefficients. This result confirms that the spatial relationship between the nanoparticle and the dendrimer does

not influence the hydrodynamic radius of the dendrimer. This eliminates the possibility, for example, that each nanoparticle is stabilized by multiple dendrimers.[34,56,57] Additional discussion of this point will be presented later.

In the case of an ideal solution composed of homogeneous center-of-mass spheres, the translational diffusion coefficient can be calculated according to the Stokes−Einstein equation after correction for the concentration of the macromolecules (eq 1).[58,59]

$$D = \frac{k_B T}{6\pi\eta_S R_h}(1 - k\varphi) \quad (1)$$

Here, k_B is the Boltzmann constant, T is the absolute temperature, η_S is the viscosity of the solvent, R_h is the hydrodynamic radius of a spherical particle, k is a constant that equals 2.1 for an ideal hard sphere,[58,59] and Φ is the volume fraction of the dendrimer in solution. In our case, because we are studying dilute concentrations,[24,25] the term $k\Phi$ can be neglected.

The viscosities of the G4-OH and G4-OH(Pd_{55}) solutions require some discussion. First, the viscosity of D_2O (at 298 K) is 1.240 mPa·s,[60,61] which is considerably higher than the value of 0.890 mPa·s for H_2O.[62] Second, the presence of salts, which are present in the G4-OH(Pd_{55}) solution, affects the viscosity of the solvent. The extent of this effect can be estimated using the Jones−Dole equation (eq 2).[63]

$$\frac{\eta}{\eta_0} = 1 + A\sqrt{c} + Bc \quad (2)$$

Here, η is the viscosity of the solvent after salt addition, η_0 is the viscosity of the pure solvent, c is the concentration of the salts, and A and B are the Jones−Dole coefficients. The A term depends on interionic forces, and the B term depends on ion−solvent interactions.[64,65] The A term can be calculated, but the B term must be determined experimentally. The ion concentration present in the G4-OH solution is negligible, but the G4-OH(Pd_{55}) solution contains both Cl^- (from the $PdCl_4^{2-}$ precursor) and $NaBO_2$ (the oxidation product of the reductant). Accordingly, the viscosity of the G4-OH(Pd_{55}) solution can be estimated using published values of the Jones−Dole coefficients for KCl and $NaBO_2$.[66] The A and B terms for KCl are 0.052 L mol^{-1} and −0.014 L mol^{-1}, for NaCl 0.062 L mol^{-1} and 0.08 L mol^{-1},[64] and for $NaBO_2$ 0.094 L mol^{-1} and 0.397 L mol^{-1}, respectively.[66] The maximum final concentration of Cl^-, assuming complete hydrolysis of $PdCl_4^{2-}$, is 2.2 mM. Due to the 2:1 stoichiometry of Cl^-:K^+ in K_2PdCl_4, we estimate the final concentration of $NaBO_2$ to be 5.5 mM. Using these values in eq 2, the calculated maximum viscosity of the G4-OH(Pd_{55}) solution is 1.254 mPa·s, which is just 1.2% higher than that of pure D_2O (1.240). Small variations in these ion concentrations will not have an appreciable influence on the solution viscosity.

The diffusion coefficients for G4-OH and G4-OH(Pd_{55}) are determined by fitting the peak-intensity decay curves of the DOSY experiments (Figure S11). In both cases, $D = (1.03 \pm 0.02) \times 10^{-10}$ m^2/s. Using eq 1, these experimentally determined diffusion coefficients, and the proper viscosities for each of the two solutions, the calculated R_h for G4-OH and G4-OH(Pd_{55}) is 1.7 ± 0.2 nm for both species. As discussed next, this experimentally determined value is smaller than a previously reported R_h for G4-NH_2 and similar to the only published value for G4-OH. Specifically, PFGSE NMR has been used to measure R_h for G4-NH_2[24] and G4-OH,[25] resulting in values of 2.08 ± 0.13 nm and ∼1.85 nm, respectively.

Methods other than PFGSE NMR have also been used to measure the size of PAMAM dendrimers. For example, small-angle X-ray scattering (SAXS) techniques[58,67−70] have been used to measure the radius of gyration (R_g) of G4-NH_2, and these values can be converted to the hydrodynamic radius: R_h = 2.1 to 3.1 nm ($R_h = R_g/(^3/_5)^{1/2}$), considering the dendrimers as nondraining hard spheres[71] and depending on the model used to interpret the experimental data. Holographic relaxation spectroscopy and dynamic light scattering measurements[72] indicate R_h = 2.66 nm for G4-NH_2. Small-angle neutron scattering (SANS) techniques have been used to study the size of G4-NH_2 at different pD's. These range from $R_h = 2.762 \pm 0.095$ nm at pD = 10.25 to 2.772 ± 0.032 nm at pD = 4.97,[73] and as in the previous case, the dendrimers are considered as nondraining hard spheres.[71] Finally, molecular dynamics (MD) simulations have generated dendrimer sizes that are in close agreement to those we determined. To directly compare these calculated values to ours, however, it was necessary to first convert the reported R_g values to R_h using the equation given earlier. Opitz et al. performed simulations in vacuum that result in a hydrodynamic radius for G4-NH_2 of 1.73 nm and found that it increases to 1.83 nm in aqueous base.[74] Other MD calculations indicate R_h values for G4-NH_2 of 1.91 nm (in aqueous base),[75] 1.87 nm[76] and 1.44 nm[77] (in the gas phase at

(56) Tanaka, H.; Koizumi, S.; Hashimoto, T.; Satoh, M.; Itoh, H.; Naka, K.; Chujo, Y. *Macromolecules* **2007**, *40*, 4327–4337.
(57) Tanaka, H.; Hashimoto, T.; Koizumi, S.; Itoh, H.; Naka, K.; Chujo, Y. *Macromolecules* **2008**, *41*, 1815–1824.
(58) Rathgeber, S.; Monkenbusch, M.; Kreitschmann, M.; Urban, V.; Brulet, A. *J. Chem. Phys.* **2002**, *117*, 4047–4062.
(59) Dhont, J. *An Introduction to the Dynamics of Colloids*; Elsevier: Amsterdam, 1996.
(60) Böhme, U.; Scheler, U. *Macromol. Chem. Phys.* **2007**, *208*, 2254–2257.
(61) Hardy, E. H.; Zygar, A.; Zeidler, M. D.; Holz, M.; Sacher, F. D. *J. Chem. Phys.* **2001**, *114*, 3174–3181.
(62) Dean, J. A. *Lange's Handbook of Chemistry*, 13rd ed.; McGraw-Hill Book Company: 1985.
(63) Jones, G.; Dole, M. *J. Am. Chem. Soc.* **1929**, *51*, 2950–2964.
(64) Jenkins, H. D. B.; Marcus, Y. *Chem. Rev.* **1995**, *95*, 2695–2724.
(65) Waghorne, W. E. *Philos. Trans. R. Soc. London, Ser. A* **2001**, *359*, 1529–1543.
(66) Cloutier, C. R.; Alfantazi, A.; Gyenge, E. *Adv. Mater. Res.* **2007**, *15−17*, 267–274.
(67) Ohshima, A.; Konishi, T.; Yamanaka, J.; Ise, N. *Phys. Rev. E* **2001**, *64*, 051808−1−051808−9.
(68) Mallamace, F.; Lesieur, P.; Lombardo, D.; Scolaro, L. M.; Romeo, A.; Romeo, E. *Prog. Colloid Polym. Sci.* **1999**, *112*, 152–156.
(69) Mallamace, F.; Canetta, E.; Lombardo, D.; Mazzaglia, A.; Romeo, A.; Scolaro, L. M.; Maino, G. *Physica A* **2002**, *304*, 235–243.
(70) Prosa, T. J.; Bauer, B. J.; Amis, E. J.; Tomalia, D. A.; Scherrenberg, R. J. *J. Polym. Sci., Part B: Polym. Phys.* **1997**, *35*, 2913–2924.
(71) Uppuluri, S.; Keinath, S. E.; Tomalia, D. A.; Dvornic, P. R. *Macromolecules* **1998**, *31*, 4498–4510.
(72) Stechemesser, S.; Eimer, W. *Macromolecules* **1997**, *30*, 2204–2206.
(73) Chen, W.-R.; Porcar, L.; Liu, Y.; Butler, P. D.; Magid, L. J. *Macromolecules* **2007**, *40*, 5887–5898.
(74) Opitz, A. W.; Wagner, N. J. *J. Polym. Sci., Part B: Polym. Phys.* **2006**, *44*, 3062–3077.
(75) Lee, I.; Athey, B. D.; Wetzel, A. W.; Meixner, W.; Baker, J. R., Jr. *Macromolecules* **2002**, *35*, 4510–4520.
(76) Maiti, P. K.; Çagin, T.; Wang, G. F.; Goddard, W. A. *Macromolecules* **2004**, *37*, 6236–6254.
(77) Çagin, T.; Wang, G. F.; Martin, R.; Breen, N.; Goddard, W. A. *Nanotechnology* **2000**, *11*, 77–84.

high pH), and 2.16 nm (in water).[78] Han et al. reported a theoretical R_h for G4-NH_2 of ~1.79 nm and $D = 1.25 \times 10^{-10}$ m^2/s.[79]

Our finding that R_h is the same for G4-OH with and without DENs strongly suggests that DENs are encapsulated by single dendrimers. This is because formation of aggregates of one or more Pd nanoparticles with multiple dendrimers would result in a higher-than-observed R_h.[34,56,57] Consider, for example, the smallest possible DSN consisting of two G4-OH PAMAM dendrimers attached to a single nanoparticle. We used two models to make an estimate of the expected diffusion coefficient of such an aggregate. One model is based on the molecular weight of the DSN, and the other is based on its shape.

To a first approximation, the molecular weight of the smallest DSN is the sum of the masses of two G4-OH dendrimers and a single nanoparticle. However, the mass of two G4-OH dendrimers is approximately the same as that for a single G5-OH dendrimer.[79] The radius of G5-OH is ~30% greater than that of G4-OH ($R_h = 1.7$ nm),[34,56,57] or ~2.2 nm, which corresponds to $D = 0.79 \times 10^{-10}$ m^2/s.

For the shape-based model, we assume that the smallest DSN aggregate has a pseudo cylindrical shape consisting of two hard spheres. Taking again 1.7 nm for the radius of the G4-OH, the cylinder has a height of 6.8 nm and a diameter of 3.4 nm. The hydrodynamic volume of such a cylinder is 62 nm^3. No correction to the Stokes−Einstein equation is required for an elongated, prolate shape if the height divided by the base is less than 3 (in this case it is 2), and therefore we can consider this cylinder to be a sphere with a volume of 62 nm^3, which corresponds to a radius of 2.5 nm.[80] The calculated diffusion coefficient of such an object would be 0.70×10^{-10} m^2/s.

Recall that the lowest value of D measured for G4-OH and G4-OH(Pd_{55}) in the PFGSE experiments is $(1.03 \pm 0.02) \times 10^{-10}$ m^2/s. Therefore, both of these hypothetical DSN models, which have values of D well below the estimates for the smallest DSNs, can be excluded. The absence of DSNs is corroborated by the ^{1}H NMR data, which indicate that there is little interaction between the terminal-group methylenes and the nanoparticle. The opposite would likely be true if multiple dendrimers were stabilized by a single nanoparticle.

Extraction of DENs. Earlier, we showed that the NMR signals arising from the inner methylene groups of G4-OH significantly decrease in the presence of DENs. We expect, therefore, that if encapsulated nanoparticles are removed from the dendrimers, the signal will recover and match that of the DEN-free dendrimer. The following experiment was designed to test this hypothesis.

We have previously shown that Pd DENs can be extracted intact from within G4-OH using alkylthiol ligands.[1] The mechanism involves adsorption of alkylthiols onto the DEN surface, which weakens the dendrimer/nanoparticle interaction and extracts the DEN as a monolayer-protected cluster (MPC).[55,81] Accordingly, a solution of G4-OH(Pd_{55}) was prepared, and the ^{1}H NMR spectrum was measured. Next, different concentrations of 2-mercaptoethanol were added to this solution, and the spectrum was measured again. At a particular threshold concentration of 2-mercaptoethanol, we expect the DENs to be extracted and therefore to observe a corresponding increase in the intensity of the inner methylene groups of the dendrimer spectrum. There is a convenient internal control for this experiment because, as discussed earlier, the NMR signals from the outer (terminal) methylenes are not significantly affected by the presence of the DENs. Therefore their intensity should be independent of the extraction process.

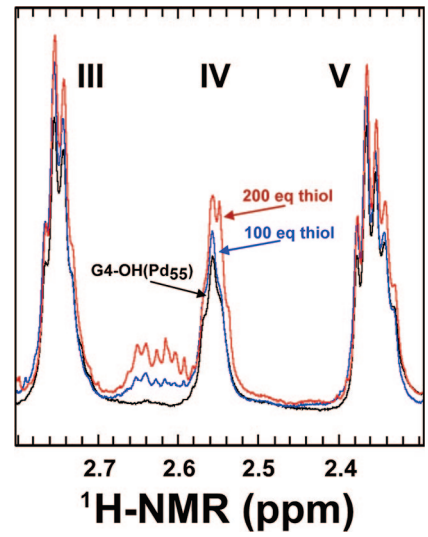

Figure 8. Expansion of ^{1}H NMR spectra for G4-OH(Pd_{55}) and after addition of (blue) 100 and (red) 200 equiv of mercaptoethanol. The figure shows the increase in the multiplet signal at 2.60 ppm and the recovery in the internal-methylene peak intensity. The spectra have been normalized to compensate for dilution arising from the addition of 2-mercaptoethanol.

Figure 8 shows ^{1}H NMR spectra of G4-OH(Pd_{55}) before and after addition of 100 and 200 equiv of 2-mercaptoethanol with respect to dendrimer concentration. Upon addition of the thiol, some of the dendrimer proton signals increase in intensity. This is especially apparent for the *a*, *d*, and *b* methylenes. Note, however, that the signal intensity does not fully regain the value of DEN-free G4-OH even after addition of 200 equiv of 2-mercaptoethanol. This might be due to incomplete DEN extraction, but addition of more mercaptoethanol complicates interpretation of the NMR data and peak integrations. This is a consequence of the presence of disulfide (oxidation product of mercaptoethanol) peaks and the severe overlap of the thiol signals with the *C*/*c* and *d* methylene signals. The key point, however, is that the increase in the intensity of the interior methylenes after addition of 2-mercaptoethanol provides corroborating evidence for the presence of DENs within the dendritic voids.

In addition to recovery of the internal methylene peak intensity, a new, broad peak is also observed at 2.6 ppm in Figure 8. This peak is attributable to the methylene protons of the alkylthiol groups now present on the Pd nanoparticles.[54] Line broadening like that observed for this peak has previously been noted for stabilizing ligands associated with other types of metal clusters, including MPCs,[1,52−55,81−84] DSNs,[85] and

(78) Maiti, P. K.; Çagin, T.; Lin, S. T.; Goddard, W. A. *Macromolecules* **2005**, *38*, 979–991.
(79) Han, M.; Chen, P.; Yang, X. *Polymer* **2005**, *46*, 3481–3488.
(80) Macchioni, A.; Ciancaleoni, G.; Zuccaccia, C.; Zuccaccia, D. *Chem. Soc. Rev.* **2008**, *37*, 479–489.
(81) Hostetler, M. J.; Zhong, C. J.; Yen, B. K. H.; Anderegg, J.; Gross, S. M.; Evans, N. D.; Porter, M.; Murray, R. W. *J. Am. Chem. Soc.* **1998**, *120*, 9396–9397.
(82) Zelakiewicz, B. S.; de Dios, A. C.; Tong, Y. Y. *J. Am. Chem. Soc.* **2003**, *125*, 18–19.
(83) Zelakiewicz, B. S.; Lica, G. C.; Deacon, M. L.; Tong, Y. Y. *J. Am. Chem. Soc.* **2004**, *126*, 10053–10058.
(84) Zelakiewicz, B. S.; Yonezawa, T.; Tong, Y. Y. *J. Am. Chem. Soc.* **2004**, *126*, 8112–8113.

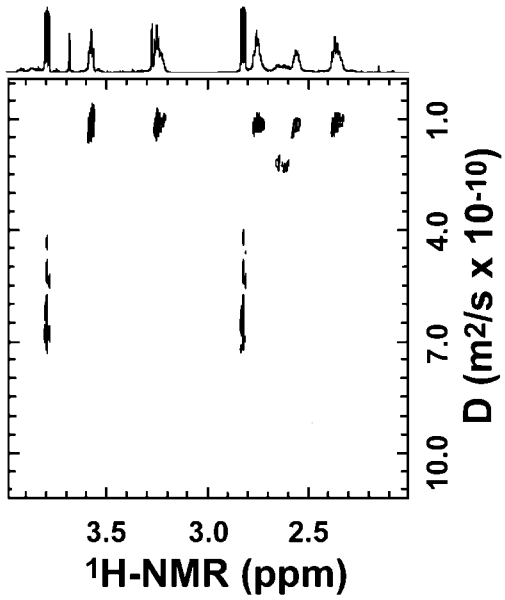

Figure 9. Pseudo-2D DOSY plot for G4-OH(Pd_{55}) after addition of 200 equiv of 2-mercaptoethanol. Signals are present for G4-OH(Pd_{55}) and for the oxidation product of 2-mercaptoethanol. New signals at 2.60 ppm, which have a diffusion coefficient higher than that for G4-OH(Pd_{55}), are also observed. This signal probably corresponds to the extracted Pd nanoparticle in the form of a monolayer-protected cluster.

nanoparticle-cored dendrimers (NCDs).[86] This peak broadening has been attributed to a decrease in the T_2 relaxation (spin−spin relaxation) and the presence of structurally different binding sites on the particle surface.[82]

To better understand the broad peak at 2.6 ppm, a PFGSE experiment was carried out using a mixture of G4-OH(Pd_{55}) and 200 equiv of 2-mercaptoethanol (Figure 9). The pseudo-2D DOSY plot is similar to that observed for G4-OH(Pd_{55}) (Figure 7), but it reveals the presence of two major species having different diffusion coefficients. One of these diffusion coefficients corresponds to G4-OH(Pd_{55}), but the one at 2.6 ppm has a slightly higher diffusion coefficient indicative of a smaller R_h. In fact, the diameter of a Pd_{55} nanoparticle is expected to be 1.1 nm, but with the mercaptoethanol monolayer it will be a little larger (but still much smaller than the dendrimer diameter of ∼3.4 nm). For example, Murray and co-workers synthesized Au MPCs having a diameter of 1.1 nm and a hexanethiolate shell.[87] They estimated the diameter of this MPC to be ∼2.7 nm.[88,89]

Summary and Conclusions

The principal result of this study is that NMR spectroscopic results are consistent with the prevailing model for DENs of a single nanoparticle contained within the void space of a single dendrimer. This conclusion is based on the following results. First, detailed analysis of the NMR data shows that signals arising from the innermost protons of G4-OH(Pd_{55}) decrease much more than signals arising from the terminal methylenes. This means that DENs are encapsulated within dendrimers rather than being adsorbed to their surface, as would be the case for DSNs. Second, extraction of the DENs as MPCs results in an increase in the NMR intensity associated with the methylenes of the branch groups, which corroborates the previous point. Third, NMR diffusion experiments demonstrate that G4-OH and G4-OH(Pd_{55}) have identical hydrodynamic radii, and this finding excludes the presence of dendrimer/nanoparticle aggregates such as DSNs.

Acknowledgment. We gratefully acknowledge the Robert A. Welch Foundation (Grant F-1288) for financial support of this project. J.G. is indebted to the Junta de Comunidades de Castilla-La Mancha (Spain) for a postdoctoral research grant. This research is also supported by a Marie Curie Intraeuropean Fellowship awarded to M.V.G., within the 6th European Community Framework Programme. A.H.V. acknowledges NanoNed for financial support. We also thank Dr. Ji-Ping Zhou of the Texas Materials Institute at UT-Austin for help with the TEM measurements. We appreciate insightful comments from Prof. Neer Asherie (Yeshiva University) regarding the interpretation of the diffusion coefficient data. The authors also acknowledge Mr. Dave Dalman (Dendritech, Inc.) for helpful discussions regarding the size of amine-terminated PAMAM dendrimers. This paper is dedicated to Professor David N. Reinhoudt on the occasion of his 66th birthday.

Supporting Information Available: $^1H-^{15}N$ HMBC and schematic correlations for different amine and amide couplings,$^1H-^{13}C$ HSQC and $^1H-^{13}C$ HMBC for G4-OH; overlapped $^1H-^{13}C$ HSQC and $^1H-^{13}C$ HMBC spectra for G4-OH; ^1H NMR spectra for G4-OH and G4-OH(Pd_{55}) and their integral values; TEM and STEM images for G4-OH(Pd_{55}) with their size-distribution histograms; $^1H-^1H$ COSY, $^1H-^{13}C$ HSQC, $^1H-^{13}C$ HMBC, and $^1H-^{15}N$ HMBC for G4-OH(Pd_{55}); T1/T2 SimFit fitting for G4-OH and G4-OH(Pd_{55}). This material is available free of charge via the Internet at http://pubs.acs.org.

JA807488D

(85) Badetti, E.; Caminade, A.-M.; Majoral, J.-P.; Moreno-Ma∼nas, M.; Sebastian, R. M. *Langmuir* **2008**, *24*, 2090–2101.
(86) Gopidas, K. R.; Whitesell, J. K.; Fox, M. A. *J. Am. Chem. Soc.* **2003**, *125*, 14168–14180.
(87) Jimenez, V. L.; Georganopoulou, D. G.; White, R. J.; Harper, A. S.; Mills, A. J.; Lee, D.; Murray, R. W. *Langmuir* **2004**, *20*, 6864–6870.
(88) Song, Y.; Jimenez, V.; McKinney, C.; Donkers, R.; Murray, R. W. *Anal. Chem.* **2003**, *75*, 5088–5096.
(89) Wolfe, R. L.; Murray, R. W. *Anal. Chem.* **2006**, *78*, 1167–1173.